IN SILICO AND *IN VITRO* EVALUATION OF SILK FIBROIN BASED AMORPHOUS BALL-MILLED BINARY SOLID DISPERSION FOR IMPROVED SOLUBILITY, DISSOLUTION AND TABLETTABILITY: THE CASE OF NAPROXEN

JIDNYASA PANTWALAWALKAR,[*] SOPAN NANGARE,[**] PRAVIN GHAGARE,[*] KISAN JADHAV[***] and NAMDEO JADHAV[*]

[*]*Department of Pharmaceutics, Bharati Vidyapeeth College of Pharmacy, Kolhapur-416013, Maharashtra state, India*
[**]*Department of Pharmaceutics, H. R. Patel Institute of Pharmaceutical Education and Research, Shirpur 425405, Dist. Dhule (MS), India*
[***]*Department of Pharmaceutics, Bharati Vidyapeeth College of Pharmacy, Navi Mumbai-400 614, Maharashtra State, India*
✉ *Corresponding author: N. R. Jadhav, nrjadhav18@rediffmail.com*

Received December 8, 2023

The present study aims to use a natural protein silk fibroin (SF) to enhance solubility, dissolution, tablettability, and subsequently, delivery of naproxen (NP) using a green technique – ball milling. The development of SF and NP solid dispersion (SF-NP-SD) for enhancing the solubility, dissolution, and compatibility of NP using ball milling. *In silico* molecular docking indicated a strong binding affinity of SF towards NP. Herein, SF-NP-SD (1:1) showed significant improvement ($p < 0.05$) in saturation solubility (12 fold) and dissolution (1.46 fold) of NP. Along with reduced wetting time ($p < 0.05$), optimum values of flowability, compressibility, and compatibility were noteworthy. The spectroscopic analysis confirmed favorable interactions, amorphization, and stabilization of NP. The tablet formulation of SF-NP-SD exhibited 1.38-fold enhanced dissolution. Molecular-level hydrophobic and hydrophilic interactions of SF favor molecular-level dispersion, enhance solubility and dissolution, and consecutively, improve drug delivery of NP.

Keywords: ball milling, dissolution, naproxen, silk fibroin, solid dispersion, solubility, tablet stability

INTRODUCTION

Silk fibroin (SF) is a natural protein-polymer obtained from the silk moth *Bombyx mori*, reared on plants.[1] Being biodegradable, biocompatible, and non-immunogenic, SF has been used traditionally and even now in modern times, for biomedical applications.[2,3] Especially, its use in textile, tissue engineering, ligatures, sutures, artificial skin, biosensing, and controlled drug delivery applications has been evident from a myriad of research findings.[4,5] Essentially, SF comprises heavy and light polypeptide chains having molecular weights of ~390 kDa and ~26 kDa, respectively.[4] The alpha helix (type I, metastable) and beta-pleated (type II, stable) conformation of SF have been extensively discussed for amorphism, crystallinity modulation, and proteinylation.[1] The typical amphiphilic nature of SF is due to $[Gly\text{-}Ala\text{-}Gly\text{-}Ala\text{-}Gly\text{-}Ser]_n$ hydrophobic repeating units, contributing to an insoluble beta-pleated crystalline form, and hydrophilic amino acids, contributing to the alpha (soluble, amorphous) form.[4,6] The annealing and proteinylation attempts have customized SF crystallinity, thus enabling its use in the formulation of nanoparticles, nanofibers, microparticles, microspheres, hydrogels *etc*., for drug delivery applications. Extensive work has been conducted in our laboratory for stabilization and novel drug delivery applications of SF.[7-12]

Solvent-based methods have been employed for the development of novel applications and formulations of SF.[1,4] However, in today's era of green technology, the utilization of renewable

resources for sustainable developments in the field of formulation science has been recommended and promoted.[13] The cost-effective, facile, less time-consuming, green technologies are a priority. In line with this, ball milling has been a prominent technology keeping abreast of aforesaid requirements.[14] Thus, it has been extensively used for mixing, size reduction (top-down), controlled structural breakdown, amorphism, *etc*. of both the actives and excipients.[13-16]

To date, various luciferous solvent-based strategies have been adopted, including wet milling, spray drying, co-amorphization, *etc*., to overcome the poor bioavailability concern of NP.[17-20] In addition, salt formation and conjugation have been investigated to improve the solubility of NP.[21-22] Reportedly, carriers, such as methylcellulose, poly(ethylene glycol) (molecular weight: 4000, 6000, 20000), *β*-cyclodextrin, gelucire, *D*-mannitol, polyvinylpyrrolidone, *etc*., have been successfully used to formulate dispersions of NP.[23-25] Reviewing prospective physicochemical properties of SF and vista of benefits offered by ball milling, the present work aims to explore solubility and dissolution improvements for NP [biopharmaceutical classification system (BCS) class II drug].[2,13] Furthermore, it was hypothesized that ball milling will impart structural breakdown of SF beta-pleated secondary structure, exposing polar side chains of hydrophilic amino acids like tyrosine, valine, and other acidic amino acids.[1,26] Importantly, these hydrophilic amino acids, along with the hydrophobic counter domains of SF, both, would contribute toward strong solid-state interactions with the structurally broken down NP. Moreover, it was assumed that NP would have a strong binding with glycine and certain hydrophilic amino acids of SF.[27,28]

To the best of our knowledge, the *in silico* molecular docking approach was employed for the first time to find the propensity of interactions between NP and SF, and the application of ligand-receptor theory for the selection of polymers in making solid dispersions (SDs). After that, the SF-NP binary SDs were prepared by ball milling, varying the ratio of SF:NP, and then evaluated for interaction intensity, percentage yield, saturation solubility, percent drug content, wettability, and *in-vitro* dissolution. The optimized SF-NP-SD was further evaluated by powder X-ray diffraction (PXRD), differential scanning calorimetry (DSC), Fourier transform infrared spectroscopy (FTIR), micromeritics, and accelerated stability study. The tablettability (compressibility and compactibility), and release performance of the optimized blend was ascertained by the Heckel and Leuenberger analysis, as well as *in-vitro* dissolution.

EXPERIMENTAL

Materials

Silk cocoons were collected from the Government Silk Processing Center, Islampur, Maharashtra, India. Naproxen was received as a gift sample from Dr. Reddy's Lab in Hyderabad, Telangana, India. Microcrystalline cellulose, HPMC (K100LV), lactose monohydrate, silicon dioxide, and magnesium stearate were purchased from Loba Chemie Pvt. Ltd., Mumbai, Maharashtra, India.

Methods

In silico *study: molecular docking analysis*

A molecular docking simulation was performed to predict possible interactions between SF and NP. A homology modeling approach was adopted to build the 3D structure of SF based on its amino acid sequence derived from *Bombyx mori*. Mainly, V. Life MDS 4.6 software was employed to construct and retrieve the appropriate structural template of SF using the FASTA file. The low-energy conformations were further optimized for the adjustment of the gradient energy to 0.001 kcal/mol/Å. Using the genetic representation of interaction patterns (GRIP) docking protocol of the Biopredicta module, all low-energy conformations within a range of 5 kcal/mol/Å from the lowest energy conformation were docked to discover ligand-receptor (SF-NP) interactions.

Extraction and characterization of SF

Initially, waste cocoon pieces were treated for 20 min with a boiling aqueous solution containing 0.5% sodium carbonate under constant stirring. The entire mass was repeatedly washed with distilled water for complete removal of sericin, followed by drying in a hot air oven.

Further, 10 g of degummed SF was dissolved in 9.3 M LiBr solution at 70 °C for 2.5 h to create the SF solution. It was succeeded by dialysis using a cellulose membrane-based dialysis cassette against distilled water for 3 days by replacing the distilled water every 6 h for complete removal of LiBr. Subsequently, the SF solution was subjected to centrifugation at 5-10 °C and 9000 rpm for 20 min. The concentrated solution was lyophilized at 0.013 mbar pressure and -49 °C temperature to obtain SF powder, which was then ground in the mortar by a pestle to obtain a uniform fine powder. Further, the UV spectrum, isoelectric pH, and percentage yield of the extracted SF were obtained to confirm its purity.[29,30]

Preparation and evaluation of SF-NP-SD

The SF-NP-SD was prepared by the ball milling technique. Accurately weighed NP and SF in the weight ratios of 1:0.5, 1:1, 1:1.5, 1:2, and 1:2.5 w/w were mixed gently and fed to a milling chamber of a ball mill having a volume of 50.27 cm^3. Further, mixtures were milled using stainless steel balls of 9 mm diameter at 100 rpm for 3 h. Then, the dispersions obtained were evaluated as described below.[30,31]

Interaction intensity

Ultraviolet-visible (UV-Vis) spectroscopy was used for the quantitative evaluation of interactions between NP and SF. All SDs (1:0.5, 1:1, 1:1.5, 1:2, and 1:2.5 w/w) were dissolved in distilled water to obtain a concentration of 10 µg/mL. The UV-Vis spectra (Shimadzu UV-1800 Spectrophotometer, Shimadzu, Japan) of all solutions were recorded in the wavelength range of 200-450 nm. The maximum absorbance of NP was measured at 235 nm and a representative factor (F) for interaction intensity was calculated using the following Equation (1):[30,32]

$$F = \frac{\text{Absorbance of the drug: fibroin SD} - \text{Absorbance of free drug}}{\text{Absorbance of free drug}} \quad (1)$$

Saturation solubility

The phase solubility method was used to calculate the saturation solubility of neat NP and SDs. A conical flask containing 20 mL of distilled water was used to dissolve an excess amount (50 mg) of plain NP and SDs (1:0.5, 1:1, 1:1.5, 1:2, and 1:2.5 w/w) and mix it using an orbital shaker for 48 h at 37 °C until equilibrium was reached. The samples were centrifuged at 7000 rpm for 10 min to ensure there was no crystalline phase from precipitation, and the supernatant was then filtered through Whatman filter paper no. 45. Additionally, materials were appropriately diluted before being examined in triplicate at 273 nm using a UV-Vis spectrophotometer (Shimadzu UV-1800 Spectrophotometer, Shimadzu, Japan).[30]

Percentage yield

The percentage yield of SD recovered from each batch (1:0.5, 1:1, 1:1.5, 1:2, and 1:2.5 w/w) was calculated by Equation (2):[30]

$$Percentage\ yield = \frac{Weight\ of\ solid\ dispersion}{Weight\ of\ drug\ and\ carrier\ mixture} \times 100 \quad (2)$$

Percent drug content

To determine the amount of drug present, precisely weighed SDs (1:0.5, 1:1, 1:1.5, 1:2, and 1:2.5 w/w), containing 10 mg of NP, were thoroughly dissolved in methanol, and NP was extracted using a sonicator for 30 min. All of the solutions were then filtered again using Whatman filter paper no. 45, diluted, and triple-tested using a Shimadzu UV-1800 Spectrophotometer (UV-Vis spectroscopy).[30]

Wettability study

In a glass funnel with an internal diameter of 3 mm, neat NP and SDs (1:0.5, 1:1, 1:1.5, 1:2, and 1:2.5 w/w), corresponding to 100 mg of NP, were added. After that, the funnel was inserted into a beaker filled with distilled water, so that the surface of the water remained level with the SDs inside the funnel. Additionally, 10 mg of methylene blue powder was uniformly put on top of the powder in the funnel, and the time needed to wet the methylene blue was recorded. The experiment was carried out three times.[30]

In-vitro *dissolution study of SF-NP-SD*

Neat NP (100 mg) and all batches of SDs (equivalent to 100 mg of NP) were evaluated for *in-vitro* dissolution using the United States Pharmacopeia (USP) Type-II apparatus, to assess an improved drug dissolution profile. The dissolution medium was 900 mL of pH 7.4 phosphate buffer. Its temperature was held constant at 37.05 °C. The paddle's rotational speed was maintained at 100 rpm. Herein, a 5 mL sample was taken from each basket every 15 min, and the same volume of fresh dissolution medium was utilized to replace the removed dissolution medium. The materials were appropriately diluted before being subjected to UV spectroscopic analysis at a maximum wavelength of 273 nm.[31] Based on the outcomes of the aforesaid, an optimized batch of SD was selected and further analyzed.

Spectroscopic characterization

The Powder X-ray diffraction (PXRD) patterns of neat SF, NP, and optimized SD were recorded on a Philips X-ray diffractometer (PW-3710, Holland) with Cu Kα radiation (λ = 1.5405 Å) at 40 kV voltage, 30 mA current, and 5×10^3 cps scanning rate. The samples were examined over a 2Θ range from 10° to 70°. Thermal analysis of SF, NP, and optimized SD was performed by differential scanning calorimetry (DSC, Mettler Toledo, Switzerland), operating with STARe software, version 5.1. For this, 5 mg of each sample was heated to a temperature of 300 °C, at a continuous rate of 10 °C/min, while being purged with dry nitrogen (80 mL/min) in aluminum pans that were pin-holed and crimped. To identify physicochemical interactions between SF, and NP, the FTIR spectra of neat SF, NP, and optimized SD were recorded using Fourier transform infrared spectroscopy (FTIR spectrophotometer, Bruker Alpha-T, India). About 2 mg of samples were placed in the sample holder and the spectra were recorded over the wavenumber range of 400-4000 cm^{-1}.

Tablettability evaluation

In this step, a ball-milled optimized batch of SD was gently passed through sieve number 18 (ASTM) and evaluated for flowability, compressibility, and compactibility. The angle of repose, Carr's

compressibility index, Hausner's ratio, Kawakita constant, Heckel plot, and Leuenberger evaluation were carried out by the equations below.[33,34] The studies were performed in triplicate.

$$Tan\theta = \frac{h}{r} \quad (3)$$

where Θ is the angle of repose, h is the height of the pile, and r is the radius of the pile.

$$Carr's\ compressibility\ index\ (\%) = \frac{Tapped\ density - Bulk\ density}{Tapped\ density} \times 100 \quad (4)$$

$$Hausner's\ ratio = \frac{Tapped\ density}{Bulk\ density} \quad (5)$$

The values of the Kawakita constants a and b, which describe the cohesive qualities and compressibility of the optimized SD, were then computed using the following Equation (6):[35]

$$\frac{N}{C} = \frac{N}{a} + \frac{1}{ab} \quad (6)$$

where N is the tapping number, and C is the degree of volume reduction.

The Heckel plot was constructed to analyze the relationship between pressure and relative density. The optimized ball-milled batch of SD was compressed using a hydraulic press (Techno Search Instruments, Mumbai, Maharashtra, India) with an 8-mm flat-faced punch and die set (lubricated with 1% w/v dispersion magnesium stearate) for 1 min of dwell time in triplicate for each ton. Compacts were given a 24-h relaxation period in ambient circumstances, after which the relative density of each applied pressure was calculated. The consolidation behavior of compacts was determined graphically and the mean yield pressure (1/k) was calculated based on the following formula:[35]

$$\ln\left[\frac{1}{1-\rho r}\right] = kP + A \quad (7)$$

where ρ_r is the relative density, k is the slope, p is the applied pressure, and A is the intercept.

The relationship between pressure and tensile strength was investigated by the Leuenberger analysis. The plot of the tensile strength (σ_t) versus pressure and relative density was constructed, and the value of compatibility (σ_{tmax}) and compression susceptibility (γ) was calculated by following Equation (8):[36]

$$\sigma_t = \sigma_{tmax}\left[1 - e^{(\gamma P pr)}\right] \quad (8)$$

where 'σ_t' is tensile strength. The study was performed in triplicate.

Accelerated stability study

The stability of optimized SD was assessed under accelerated conditions of relative humidity (75% RH ± 5% RH) and temperature (40 ± 2 °C) as per ICH guidelines. The SD was placed in a stability chamber for 3 months. Samples were withdrawn every month from the time of placing up to 3 months and further analyzed by FTIR, PXRD, and *in-vitro* dissolution.

Formulation and* in-vitro *dissolution of tablets

Optimized SD was formulated into tablets by the direct compression method using a tablet press (a 10-station Minipress, Karnawati Engineering, Mehsana, Gujrat, India) having 8 mm die and flat-faced punch. The microcrystalline cellulose, silicon dioxide, HPMC (K100LV), and magnesium stearate (Table 1) were used as ingredients, and tablet hardness was adjusted to 5 kg/cm^2. The prepared tablets were allowed to relax for 24 h at ambient conditions and further evaluated for *in-vitro* dissolution using USP type-II dissolution test apparatus in phosphate buffer of pH 7.4 under the following conditions: temperature: 37 ± 0.5 °C, paddle speed: 50 rpm, 5 mL of sample withdrawn and replaced by the same volume of fresh buffer medium. The withdrawn samples were filtered, suitably diluted, and analyzed by a UV-Vis spectrophotometer at the wavelength maximum of 273 nm.[37] The dissolution profile of SD tablets was compared with conventional tablets containing neat NP, and the similarity factor (f_2), the difference factor (f_1), and p-value were calculated.[33]

Ligand–receptor interaction analysis

To ascertain the interaction of NP with SF (ligand-recepto– binding), an *in-silico* study was performed. Reportedly, NP binds with the glycine residue of the cyclooxygenase enzyme, whilst glibenclamide binds with serine at the pancreatic K_{ATP} channel. As glycine and serine are the chief constituents of SF and sericin, respectively, the co-amorphous systems of glibenclamide-serine (1:1) and NP-glycine (1:1) were prepared by ball milling technique (milling cylinder volume – 50.27 cm^3, speed –100 rpm, time – 3 h) and evaluated for interaction intensity. To validate the interaction hypothesis, SDs of SF-NP, NP-sericin, glibenclamide-SF, and glibenclamide-sericin were prepared by the ball milling technique and evaluated for interaction intensity and *in-vitro* dissolution. Finally, f_1 and f_2 were calculated.[30]

Statistical analysis

Statistical significance was tested by the Analysis of Variance (ANOVA) at a 95% confidence interval. The paired '*t*' test was performed.

RESULTS AND DISCUSSION

Initially, SF extracted from the waste silk cocoons of *Bombyx mori* showed a UV absorption band at 276 nm and isoelectric pH at 4.2. The percentage yield of SF was found to be 79.10 wt%. All the values were in agreement with the literature reports, confirming the purity of extracted SF.[33]

***In silico* study: molecular docking analysis**

The output of virtual molecular level interactions between NP and SF has been depicted in Figure 1. The docking score (binding energy) of SF-NP was found to be -54.50.

Further, NP was found to be interacting with SF via a hydrogen bond with Glu28B. Aromatic interactions were observed with Phe84A, Phe26B, and Phe26B, whereas charge interactions were reported with Lys63B and Glu28B. The hydrophobic interactions were also noted with the glycine, as anticipated. The confirmation of virtual interactions could plausibly explain the wet laboratory findings, as well.

Table 1
Tablet formulation composition for SF-NP-SD

Ingredients	Quantity (mg)
Solid dispersion (1:1)	150
Microcrystalline cellulose	45
HPMC (K 100LV)	75
Silicon dioxide	5
Magnesium stearate	5
Total weight	400

Figure 1: Molecular docking interaction for SF-NP

Preparation and evaluation of SF-NP- SDs

The processability of all batches of SDs was optimum and could generate the desired SDs. The evaluation outcome of SDs has been given below.

Interaction intensity

The highest interaction intensity (0.85 ± 0.04) was observed in SD comprising a NP to SF ratio of 1:1, followed by those with the ratios of 1:0.5 (0.70 ± 0.03), 1:1.5 (0.67 ± 0.03), 1:2 (0.65 ± 0.02), and 1:2.5 (0.63 ± 0.02). This could reveal that SF incorporation increased the absorption intensity of NP, without any significant shift in λ_{max}. Also, no deviation of the spectrum from the baseline was observed, confirming enhanced absorption intensity, and excluding the absorbance of SF. Still, the interaction intensity of SD (1:1) was significantly different ($p < 0.05$) than those for the remaining ratios of NP:SF.

Saturation solubility of NP

The saturation solubility of neat NP was found to be 0.08 ± 0.004 mg/mL. All SDs (1:0.5, 1:1, 1:1.5, 1:2, and 1:2.5 w/w) had significantly enhanced saturation solubility ($p < 0.05$), over that of neat NP. Especially, SD (1:1) showed the highest saturation solubility (12 fold higher than that of neat NP), *i.e.* 0.98 ± 0.048 mg/mL, followed by 1:0.5 (0.82 ± 0.040 mg/mL), 1:1.5 (0.79 ± 0.037 mg/mL), 1:2 (0.76 ± 0.035 mg/mL) and 1:2.5 (0.74 ± 0.033 mg/ mL). The presence of SF did not exhibit any interference.

Percentage yield and percent drug content

The percentage yield of SDs (1:0.5, 1:1, 1:1.5, 1:2, and 1:2.5 w/w) was found to be in the range from 85.47 ± 2.16% to 93.72 ± 2.76%, as given in Table 2. The highest yield was found in the SD comprising a 1:1 ratio of NP and FD. The SD

(1:1) showed maximum drug content (98.30 ± 1.53%). However, the drug content gradually decreased in SDs in the order (1:0.5, 1:1.5, 1:2, 1:2.5), respectively (Table 2).

Wettability study

The average wetting time required for pure NP was found to be 50.82 ± 2.51 seconds. As seen in Table 2, all the compositions of SDs showed less wetting time compared to pure NP. Amongst all batches of SDs, SD (1:1) exhibited the lowest wetting time (38.19 ± 1.85 s). A statistically significant difference was noted between the wetting time of plain SF and SD (1:1) at $p < 0.05$. Hence, it could be confirmed that SF-based ball-milled binary SDs can be used to improve SF and NP wettability.

Table 2
Percentage yield, percent drug content, and wetting time for SDs prepared at various SF:NP ratio

SF-NP-SD ratio	Percent yield	Percent drug content	Wetting time (s)
1:0	-	-	50.82±2.51
1:0.5	91.14±2.25	94.29 ±1.77	39.46±1.93
1:1	93.72±2.76	98.30 ± 1.53	38.19±f1.85
1:1.5	88.26±2.49	91.85 ± 1.89	40.94±1.96
1:2	87.35±2.21	89.62 ± 1.81	41.20±2.11
1:2.5	85.47±2.16	88.30 ± 1.57	42.13±2.13

*All readings are average ± SD (n=3)

***In-vitro* dissolution study**

The *in-vitro* dissolution profiles of NP and all batches of SDs have been depicted in Figure 2. Herein, NP showed comparatively less dissolution (63.47 ± 3.11%) in phosphate buffer pH 7.4 at the end of 60 min. It was observed that all batches of SDs showed significant improvement ($p < 0.05$) in the dissolution profile of NP. The maximum dissolution was observed in SD 1:1 (93.21 ± 4.47%), followed by SD 1:0.5 (90.17 ± 4.23%), SD 1:1.5 (88.64 ± 4.03%), SD 1:2 (87.91 ± 3.61%), and SD 1:2.5 (85.54 ± 3.51%). Thus, SD 1:1 demonstrated a 1.46-fold improved dissolution, compared to neat NP. Considering the aforementioned outcomes, SD (1:1) was selected as an optimized batch and analyzed further.

Spectroscopic characterizations

The diffractogram of NP exhibited numerous high-intensity diffraction peaks at 2Θ values of 12.23°, 16.04°, 17.94°, 21.84°, 22.26°, 23.70°, 25.54°, 27.41°, and 33.41°, confirming its crystalline nature. The absence of characteristic high-intensity peaks in the SF diffractogram revealed its amorphous nature. As depicted in Figure 3, the diffractogram of SD (1:1) showed a disappearance of the crystallinity peaks corresponding to the amorphous form of NP in SD.

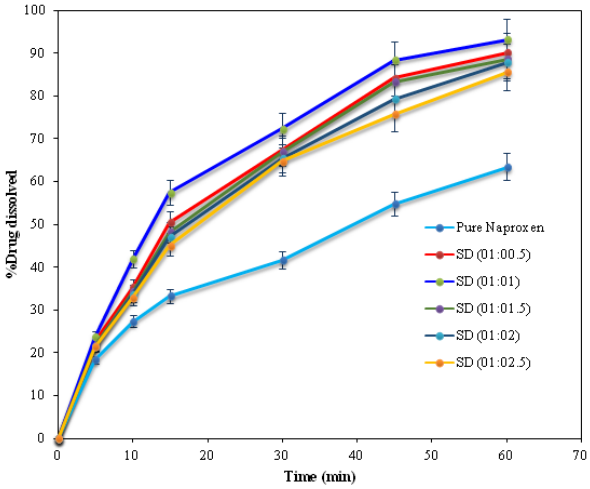

Figure 2: *In-vitro* dissolution profile of pure naproxen and SDs at various SF:NP ratios

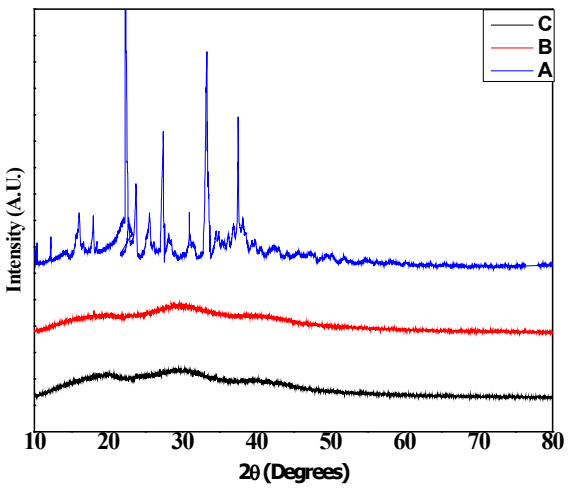

Figure 3: Powder X-ray diffraction patterns for (A) NP, (B) SF, and (C) SF-NP-SD (1:1)

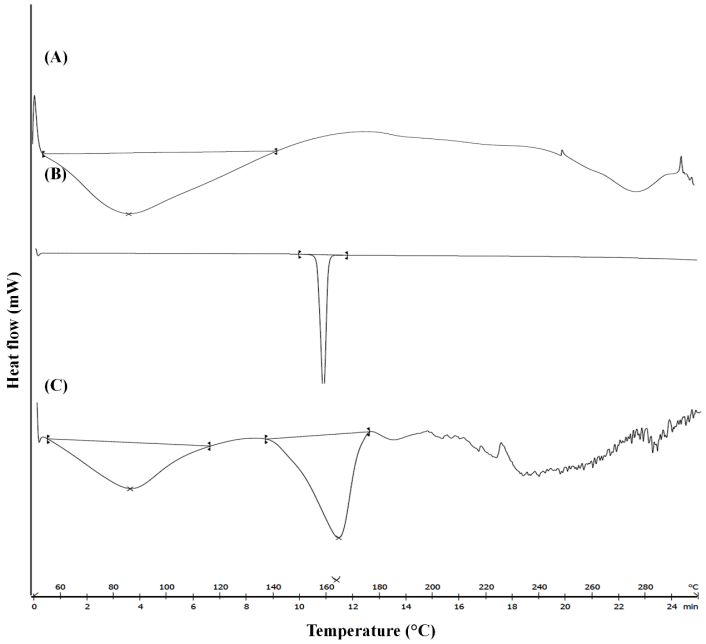

Figure 4: DSC thermograms for (A) SF, (B) NP, and (C) SF-NP-SD (1:1)

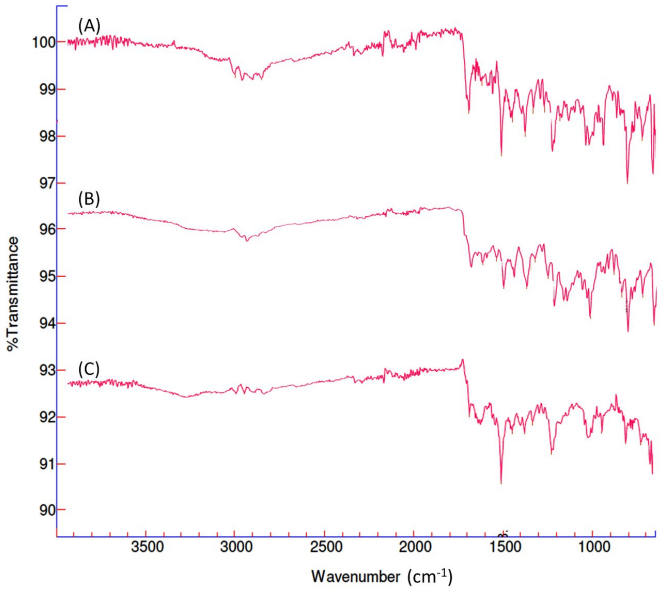

Figure 5: FTIR spectra of (A) NP, (B) SF, and (C) SF-NP-SD (1:1)

The DSC thermogram of neat NP showed a sharp endothermic peak at 156.75 °C, signifying the melting point of the crystalline form. SF showed the presence of a broad endothermic peak at 86.77 °C, owing to its moisture content, followed by another endothermic peak at 285 °C, depicting its amorphous nature. The presence of two endothermic peaks observed in the DSC thermogram of SD (1:1) corresponded to the melting of SF (85.35°C) and NP (163.56°C) respectively, along with the strong intermolecular adhesive interactions. The broad endothermic peaks signified the disruption of crystallinity, revealing amorphous form/molecular dispersion of NP in the SF matrix, as evident from Figure 4.

The FTIR spectra of neat NP, SF, and SD (1:1) have been depicted in Figure 5. In the spectra, neat NP could enunciate prominent peaks at wavenumbers of 1228.46 cm^{-1}, 1273.45 cm^{-1}, 1690.45 cm^{-1}, and 2833.73 cm^{-1}, representing C-O stretching vibration (ether), C-O stretching vibration (acid), C-C aromatic stretching

vibration, and C-H aliphatic stretching vibration, respectively. SF exhibited characteristic peaks at wavenumbers of 1685.24 cm^{-1} – amide I (C=O stretching vibration), 1508.58 cm^{-1} – amide II (N-H bending vibration), and 1379.39 cm^{-1} – amide III (C-N stretching vibration). The FTIR spectra of SD (1:1) displayed a shift of principal peaks of NP to lower wavenumbers, with reduced intensity at 1227.82 cm^{-1} (C-O stretching vibration), 1685.22 cm^{-1} (C-C aromatic stretching vibration), and 2832.51 cm^{-1} (C-H aliphatic stretching vibration). This indicated a good degree of interaction between NP and SF. Furthermore, the broadening of characteristic peaks of NP confirmed amorphization and its molecular-level interactions.

Tablettability evaluation

The SF-NP-SD (1:1) could demonstrate the value of the angle of repose, Carr's compressibility index, and Hausner's ratio to be 29.48° ± 1.28°, 8.52 ± 2.13, and 1.09 ± 0.05, respectively, indicating excellent flowability over that of neat NP. The Kawakita plot revealed excellent flowability, as signified by a lower value of the Kawakita constant a = 0.31 ± 0.03, and a high value of constant b = 0.74 ± 0.05, indicating better compression. The value of mean yield pressure, Py = 0.94 ± 0.05, could reveal excellent consolidation and better compressibility of SD. Meanwhile, as per Leuenberger's analysis, the values of σ_{tmax} and γ, found to be 10.04 ± 1.16 and 3.49 ± 0.63, respectively, for SD (1:1) in tabletted form, could signify excellent compactibility. Thus, excellent flowability, better compressibility, and compactibility were revealed for the SDs.

Accelerated stability study

Herein, the presence of an amorphous form of NP under accelerated conditions could be attributed to the disruption of its crystallinity and strong molecular-level interactions with the SF. After 3 months of accelerated stability study (Fig. 6), it was observed that SF inhibited the devitrification of NP completely. It means that ball milling induced crystallinity disruption of NP, further leading to amorphism and its stabilization by SF. The FTIR spectra of the stability study samples showed decreased peak intensities, with a slight broadening of peaks, indicating complete amorphization of NP, as depicted in Figure 7. This confirmed that SF suppressed the recrystallization of NP efficiently even under accelerated conditions of temperature and humidity.

The *in-vitro* dissolution study of SD (1:1) showed enhanced dissolution of NP for all conditions of the accelerated stability study. The drug dissolution was not significantly affected by the accelerated conditions. The percent dissolution was found to be 93.21 ± 4.47%, 92.46 ± 1.38%, 92.12 ± 1.72%, 91.85 ± 1.32% in phosphate buffer of pH 7.4 on days 0, 30, 60 and 90, respectively. A consistent dissolution profile with an insignificant difference (p < 0.05) confirmed the amorphous form of the NP, even after the accelerated stability study.

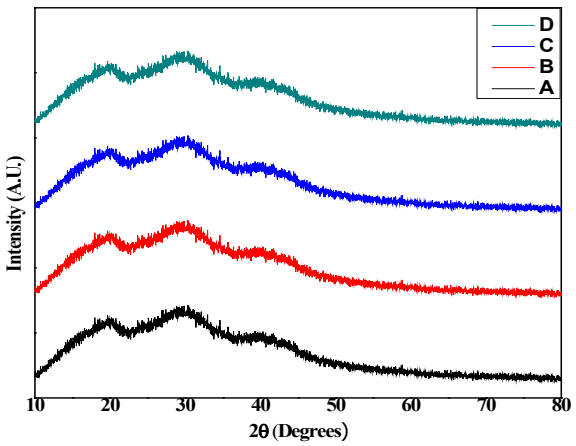

Figure 6: Accelerated stability study diffractogram for days (A) 0, (B) 30, (C) 60, and (D) 90

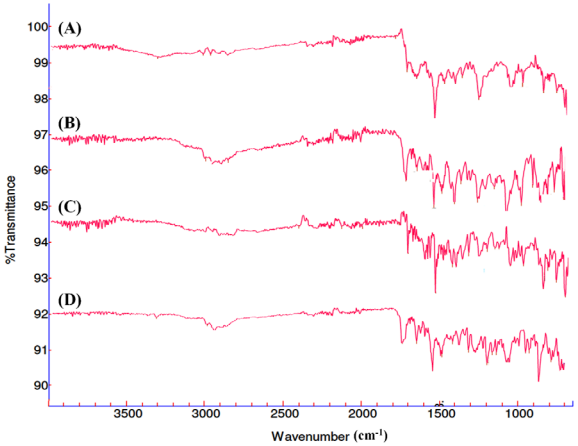

Figure 7: FTIR spectra for stability study samples on days (A) 0, (B) 30, (C) 60, and (D) 90

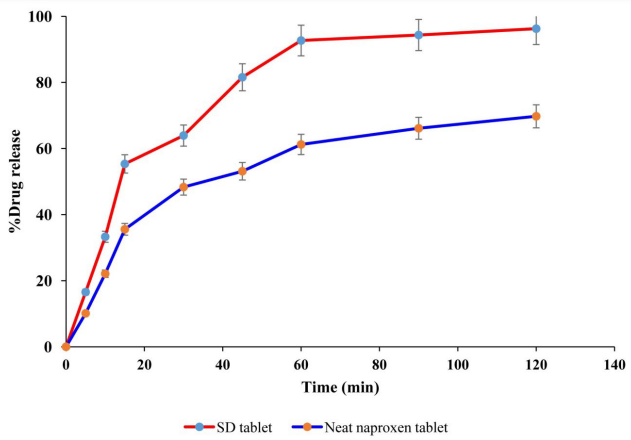

Figure 8: *In-vitro* dissolution profile of SD (1:1) tablet formulation and neat NP tablet formulation

Formulation and *in-vitro* dissolution of tablets

The *in-vitro* dissolution study demonstrated 90.26 ± 3.96% dissolution of tabletted SF-NP-SDs in phosphate buffer of pH 7.4 at the end of 2 h (Fig. 8). This could confirm significant improvement (1.38 fold) in the dissolution of tabletted NP in SD, compared to the neat NP tablets. The values of f_1 and f_2 were found to be 45 and 34, respectively. Herein, the *P*-value was found to be 0.00000003 ($p < 0.05$). This could confirm significant improvement (1.38 fold) in the dissolution of tabletted NP in SD, compared to that of the neat NP tablets. Enhanced dissolution could be attributed to molecular-level hydrophobic and hydrophilic interactions between SF and NP, favoring molecular-level dispersion and amorphization of the NP.

Ligand-receptor interaction analysis

Interaction intensity

As hypothesized, the interaction intensity of NP-glycine was found to be maximum (0.92 ± 0.04). In addition, the interaction intensity observed for NP-SF was higher (0.85 ± 0.04), compared to that of NP-sericin (0.10 ± 0.02). In the case of glibenclamide as a drug, glibenclamide-serine demonstrated the highest interaction intensity (0.76 ± 0.03). The interaction intensity of glibenclamide-sericin and glibenclamide-SF was found to be 0.62 ± 0.03 and 0.17 ± 0.02, respectively. However, a *vice versa* relation cannot be observed, as anticipated from the ligand-receptor binding theory. The hypothesis proposed has been confirmed, underlining the role of the same in the selection of protein polymer for better interactions with the drug.

In-vitro *dissolution study*

The neat NP, SF-NP-SD, and NP-sericin SD showed 63.47 ± 3.11%, 93.21 ± 4.47%, and 66.45 ± 3.38% NP dissolution, respectively (Table 3). The f_1 and f_2 were found to be 4.95 and 80.97, respectively, depicting identical dissolution profiles of pure NP and NP-sericin-SD. Meanwhile, f_1 and f_2 values were found to be 68 and 30.89 after comparison of dissolution profiles of NP and SF-NP-SD, confirming significant variation.

Table 3
In-vitro dissolution data for SF-NP-SD in buffer of pH 7.4

Time (min)	% Drug dissolved in buffer pH 7.4					
	Neat NP	SF-NP-SD	NP-Sericin SD	Neat Glibenclamide	Glibenclamide-SF-SD	Glibenclamide-Sericin SD
0	0	0	0	0	0	0
5	18.30±0.89	23.71±1.17	15.43±0.75	11.76±0.57	17.76±0.87	21.41±1.04
10	27.35±1.36	41.91±1.91	24.39±1.18	23.89±1.14	27.89±1.36	37.41±1.79
15	33.2±1.49	57.42±2.34	34.32±1.61	29.85±1.43	38.85±1.85	52.20±2.61
30	41.67±1.95	72.29±3.48	42.67±1.96	39.12±1.87	45.12±2.21	68.89±3.30
45	54.8±2.31	88.32±4.23	55.81±2.73	47.19±2.26	58.19±2.79	81.85±4.01
60	63.47±3.11	93.21±4.47	69.45±3.38	59.28±2.84	71.38±3.49	87.36±4.33

*All readings are average ± SD (n=3)

A statistically significant difference ($p < 0.05$) was observed for % drug dissolved between neat NP and SF-NP-SD, neat glibenclamide and glibenclamide-sericin-SD; a statistically insignificant difference ($p < 0.05$) was observed for % drug dissolved between neat NP and NP-sericin-SD, neat glibenclamide and glibenclamide-SF-SD.

Enhanced dissolution of NP from SF-NP-SD could be due to higher-order interactions, indicating stronger molecular level interactions, chiefly between NP and glycine, glutamic acid, lysine, and phenylalanine. Also, glibenclamide-sericin SD (87.36 ± 4.33%) showed higher dissolution, compared to glibenclamide-SF-SD (71.38 ± 3.49%), and neat glibenclamide (59.28 ± 2.84%), because of abundant serine in sericin, facilitating stronger molecular interactions between glibenclamide and sericin. The f_1 and f_2 were found to be 14.86 and 63.82, respectively, after comparing the dissolution profile of neat glibenclamide and glibenclamide-SF-SD, suggesting similarity in dissolution profiles. Meanwhile, f_1 and f_2 were found to be 69.88 and 30.03, respectively, which assured a significant difference in the dissolution profile of pure glibenclamide and glibenclamide-sericin-SD. Thus, it confirmed the strong interactions between SF and NP.

In the contemporary research, the adoption of green technologies by employing renewable resources has gained high interest due to a multitude of advantages.[13] In line with this, we prepared SF-NP-SD by utilizing ball milling as a green technique and SF as a natural protein.[3,26] Nowadays, the *in silico* approach is widely adopted by researchers to curtail the intensiveness of laboratory work and bring smartness. Virtual screening indicated a strong binding affinity of NP towards SF, confirming the ligand-receptor binding hypothesis. This could be attributed to the abundant presence of receptor amino acids, such as glycine, lysine, phenylalanine and glutamine, in SF.[38,39] The aforesaid hypothesis can be extended in the selection of protein polymer for the preparation of SDs. Moreover, the interaction intensity analysis revealed the presence of comparatively stronger interactions between NP and SF at the ratio of 1:1, which could imply a strong impact of SF on the physicochemical properties of NP.[30] Also, the enhanced solubility of NP in SDs could be attributed to the structural breakdown of NP and stronger interactions between NP and FD.[40] The reduction in the wetting time could be attributed to the enhanced surface area of NP in the SD and hydrogen bonding, exposure of hydrophilic domains of SF on ball milling, as predicted virtually, which consecutively enhanced *in vitro* dissolution.[15,41-43] In addition, the spectroscopic analysis and the accelerated stability study showed a reduction of crystallinity peaks in XRD, broadening of the endothermic peak in DSC, and shifting of characteristic peaks to lower wavenumbers in FTIR, assuring amorphization and stabilization of NP.[30,44,45] The optimum values of angle of repose, Carr's compressibility index, and Hausner's ratio concluded better flowability of SF-NP-SD.[46] Also, the Kawakita and Leuenberger analyses assured improved tablettability of SF-NP-SD.[34,35] Overall, the SD-based tablet exhibited better dissolution, compared to the neat NP tablet. Interestingly, as glycine is present abundantly in SF, it showed better interaction intensity in SD comprising NP and SF. Glibenclamide showed better interaction intensity in SD comprising sericin. This could be due to the abundance of serine in sericin, unlike SF. Conclusively, it can be stated that glycine strongly binds with NP, thus with SF; serine strongly binds with glibenclamide, thus with sericin. As anticipated from the ligand-receptor binding theory, the hypothesis proposed has been confirmed.[47]

CONCLUSION

The successful use of ball milling, a green technology, has been made in preparing SF-based binary solid dispersions of NP. The SF-NP-SD has been explored for improving solubility, dissolution, and tablettability. The strong binding affinity of NP towards SF was confirmed by *in silico* molecular docking studies. Prepared SF-NP-SD demonstrated enhanced saturation solubility and dissolution of NP. The optimized SD (1:1) showed the highest yield, maximum drug content, reduced wetting time, highest solubility, and dissolution. The XRD, DSC, and FTIR findings confirmed the transformation of the crystalline form of NP into an amorphous form, and its simultaneous stabilization, reiterating the same in accelerated stability studies. The Heckel and Leuenberger analyses confirmed the excellent compressibility and compactibility of SF-NP-SD. The role of glycine and the secondary structure of SF towards the favorable interactions with the NP have been

delineated. Further, the interaction analysis confirmed that the ligand-receptor binding theory can be utilized to modify the physicochemical properties of drugs and select protein polymers in preparing SD. Also, the same can be extended to predict molecular level interactions deciphering amorphous form stabilization of drugs. Conclusively, the role of SF as a solubility and dissolution enhancer, along with an amorphous form stabilizer for NP, demonstrating excellent tablettability, has been established.

ACKNOWLEDGMENTS: The authors acknowledge Bharati Vidyapeeth College of Pharmacy, Kolhapur (India) for providing research facilities.

REFERENCES

[1] T. Chakraborty, A. Sarma and M. K. Das, *Curr. Trends Pharm. Res.*, **3**, 45 (2016), https://dibru.ac.in/wp-content/uploads/2020/02/Vol_3_Issue_1_A41.pdf?2023120805

[2] N. Singh, S. P. Gautam, H. Harjaskaran, A. Amanjot, L. Singh *et al.*, *Ars. Pharm.*, **57**, 137 (2016), https://doi.org/10.30827/ars.v57i3.5331

[3] C. Lujerdean, G. M. Baci, A. A. Cucu and D. S. Dezmirean, *Insects*, **13**, 286 (2022), https://doi.org/10.3390/insects13030286

[4] T. Dyakonov, C. H. Yang, D. Bush, S. Gosangari, S. Majuru *et al.*, *J. Drug. Deliv.*, **2012**, 490514 (2012), https://doi.org/10.1155/2012/490514

[5] A. Benvidi, Z. Abbasi, M. D. Dehghan Tezerjani, M. Banaei, H. R. Zare *et al.*, *Acta Chim. Slov.*, **65**, 278 (2018), https://doi.org/10.17344/acsi.2017.3667

[6] T. Asakura, *Molecules*, **26**, 3706 (2021), https://doi.org/10.3390/molecules26123706

[7] S. Dugam, S. Nangare, A. Gore, S. Wairkar, P. Patil *et al.*, *Int. J. Polym. Mater. Polym. Biomater.*, **71**, 1393 (2022), https://doi.org/10.1080/00914037.2021.1981318

[8] Y. Shen, X. Wang, B. Li, Y. Guo and K. Dong, *Int. J. Biol. Macromol.*, **211**, 514 (2022), https://doi.org/10.1016/j.ijbiomac.2022.05.064

[9] S. Nangare, S. Dugam, P. Patil, R. Tade and N. Jadhav, *Nanotechnology*, **32**, 035101 (2021), https://doi.org/10.1088/1361-6528/abb8a9

[10] T. K. Mwangi, R. D. Bowles, D. M. Tainter, R. D. Bell, D. L. Kaplan *et al.*, *Int. J. Pharm.*, **485**, 7 (2015), https://doi.org/10.1016/j.ijpharm.2015.02.059

[11] J. Pantwalawalkar and S. Nangare, *Ind. J. Pharm. Educ. Res.*, **56**, 396 (2022), https://doi.org/10.5530/ijper.56.2.59

[12] Q. Min, D. Tian, Y. Zhang, C. Wang, Y. Wan *et al.*, *Biomimetics* (*Basel*), **7**, 41 (2022), https://doi.org/10.3390/biomimetics7020041

[13] C. C. Piras, S. Fernández-Prieto and W. M. De Borggraeve, *Nanoscale Adv.*, **1**, 937 (2019), https://doi.org/10.1039/c8na00238j

[14] Z. H. Loh, A. K. Samanta and P. W. S. Heng, *Asian J. Pharm. Sci.*, **10**, 255 (2015), https://doi.org/10.1016/j.ajps.2014.12.006

[15] K. Ramadhan and T. J. Foster, *J. Food Eng.*, **229**, 50 (2018), https://doi.org/10.1016/j.jfoodeng.2017.10.024

[16] M. Mattonai, D. Pawcenis, S. S. Del Seppia, J. Łojewska and E. Ribechini, *Bioresour. Technol.*, **270**, 270 (2018), https://doi.org/10.1016/j.biortech.2018.09.029

[17] S. Kumar and D. J. Burgess, *Int. J. Pharm.*, **466**, 223 (2014), https://doi.org/10.1016/j.ijpharm.2014.03.021

[18] N. Al-Zoubi, F. Odeh, I. Partheniadis, S. Gharaibeh and I. Nikolakakis, *Pharm. Dev. Technol.*, **26**, 193 (2021), https://doi.org/10.1080/10837450.2020.1853769

[19] A. Beyer, H. Grohganz, K. Löbmann, T. Rades and C. S. Leopold, *Int. J. Pharm.*, **526**, 88 (2017), https://doi.org/10.1016/j.ijpharm.2017.04.011

[20] A. W. Lim, K. Löbmann, H. Grohganz, T. Rades and N. Chieng, *J. Pharm. Pharmacol.*, **68**, 36 (2016), https://doi.org/10.1111/jphp.12494

[21] Q. Fu, H.-D. Lu, Y.-F. Xie, J. Liu, Y. Han *et al.*, *J. Mol. Struct.*, **1185**, 281 (2019), https://doi.org/10.1016/j.molstruc.2019.02.104

[22] M. A. Hussain, I. Shad, I. Malik, F. Amjad, M. N. Tahir *et al.*, *Arab. J. Chem.*, **13**, 5717 (2020), https://doi.org/10.1016/j.arabjc.2020.04.010

[23] V. Nagabandi, A. K. Chandragiri and S. Thota, *J. Pharm. Sci. Res.*, **6**, 78 (2014), https://www.jpsr.pharmainfo.in/Documents/Volumes/vol6issue02/jpsr06021404.pdf

[24] A. Paudel, J. Van Humbeeck and G. Van den Mooter, *Mol. Pharm.*, **7**, 1133 (2010), https://doi.org/10.1021/mp100013p

[25] M. G. Rao, R. Suneetha and P. S. Reddy, *Ind. J. Pharm. Sci.*, **67**, 26 (2005)

[26] R. Rajkhowa, X. Hu, T. Tsuzuki, D. L. Kaplan and X. Wang, *Biomacromolecules*, **13**, 2503 (2012), https://doi.org/10.1021/bm300736m

[27] K. C. Duggan, M. J. Walters, J. Musee, J. M. Harp, J. R. Kiefer *et al.*, *J. Biol. Chem.*, **285**, 34950 (2010), https://doi.org/10.1074/jbc.M110.162982

[28] Y. Qi, H. Wang, K. Wei, Y. Yang, R. Y. Zheng *et al.*, *Int. J. Mol. Sci.*, **18**, 237 (2017), https://doi.org/10.3390/ijms18030237

[29] S. Faragò, G. Lucconi, S. Perteghella, B. Vigani, G. Tripodo *et al.*, *Pharm. Dev. Technol.*, **21**, 453 (2016), https://doi.org/10.3109/10837450.2015.1022784

[30] N. H. Salunkhe, N. R. Jadhav, H. N. More and A. D. Jadhav, *Int. J. Biol. Macromol.*, **107**, 1683 (2018), https://doi.org/10.1016/j.ijbiomac.2017.10.035

[31] M. Acharya, S. Mishra, R. N. Sahoo and S. Mallick, *Acta Chim. Slov.*, **64**, 45 (2017), https://doi.org/10.17344/acsi.2016.2772

[32] E. Karavas, G. Ktistis, A. Xenakis and E. Georgarakis, *Eur. J. Pharm. Biopharm.*, **63**, 103 (2006), https://doi.org/10.1016/j.ejpb.2006.01.016
[33] P. Rathod, H. More, S. Dugam, P. Velapure and N. Jadhav, *J. Pharm. Innov.*, **16**, 226 (2021), https://doi.org/10.1007/s12247-020-09440-6
[34] H. Y. Saw, C. E. Davies, A. H. J. Paterson and J. R. Jones, *Procedia Eng.*, **102**, 218 (2015), https://doi.org/10.1016/j.proeng.2015.01.132
[35] S. S. Prakash, C. N. Patra and C. Santanu, *Iranian J. Pharm. Res.*, **10**, 393 (2011), https://pubmed.ncbi.nlm.nih.gov/24250371/
[36] S. P. Singh, C. Patra and S. C. Dinda, *Trop. J. Pharm. Res.*, **11**, 387 (2012), https://doi.org/10.4314/tjpr.v11i3.7
[37] N. Maclean, I. Khadra, J. Mann, H. Williams, A. Abbott *et al*., *Int. J. Pharm. X*, **4**, 100106 (2022), https://doi.org/10.1016/j.ijpx.2021.100106
[38] C. Z. Zhou, F. Confalonieri, M. Jacquet, R. Perasso, Z. G. Li *et al*., *Proteins*, **44**, 119 (2001), https://doi.org/10.1002/prot.1078
[39] S. Puspita, S. Sunarintyas, C. Anwar, E. Mulyawati and M. Soesatyo, *BIO Web Conf.*, 2**8** (2020), https://doi.org/10.1051/bioconf/20202802001
[40] S. Alshehri, S. S. Imam, A. Hussain, M. A. Altamimi, N. K. Alruwaili *et al*., *Drug Deliv.*, **27**, 1625 (2020), https://doi.org/10.1080/10717544.2020.1846638
[41] Z. Ling, T. Wang, M. Makarem, M. Santiago Cintrón, H. N. Cheng *et al*., *Cellulose*, **26**, 305 (2019), https://doi.org/10.1007/s10570-018-02230-x
[42] A. Modi and P. Tayade, *AAPS PharmSciTech.*, **7**, 68 (2006), https://doi.org/10.1208/pt070368
[43] D. N. Bikiaris, *Exp. Opin. Drug Deliv.*, **8**, 1501 (2011), https://doi.org/10.1517/17425247.2011.618181
[44] K. Adibkia, M. Barzegar-Jalali, H. Maheri-Esfanjani, S. Ghanbarzadeh, J. Shokri *et al*., *Powder Technol.*, **246**, 448 (2013), https://doi.org/10.1016/j.powtec.2013.05.044
[45] T. T. D. Tran and P. H. L. Tran, *Pharmaceutics*, **12**, 745 (2020), https://doi.org/10.3390/pharmaceutics12080745
[46] M. Qushawy, A. Nasr, S. Swidan and Y. Mortagi, *Sci. Pharm.*, **88**, 52 (2020), https://doi.org/10.3390/scipharm88040052
[47] J. X. Wu, D. Ding, M. Wang, Y. Kang, X. Zeng *et al*., *Protein Cell.*, **9**, 553 (2018), https://doi.org/10.1007/s13238-018-0530-y